

1 **Meteorological impacts on the unexpected ozone pollution in coastal cities of China**
2 **during the unprecedented hot summer of 2022**

3 **Xiaoting Ji^{1,2,3}, Gaojie Chen^{1,2,3}, Jinsheng Chen^{1,2*}, Lingling Xu^{1,2}, Ziyi Lin^{1,2,3}, Keran**
4 **Zhang^{1,2,3}, Xiaolong Fan^{1,2}, Mengren Li^{1,2}, Fuwang Zhang⁴, Hong Wang⁵, Zhi Huang⁶,**
5 **Youwei Hong^{1,2,3*}**

6 ¹Center for Excellence in Regional Atmospheric Environment, Institute of Urban Environment,
7 Chinese Academy of Sciences, Xiamen 361021, China

8 ²Fujian Key Laboratory of Atmospheric Ozone Pollution Prevention, Chinese Academy of
9 Sciences, Xiamen 361021, China

10 ³University of Chinese Academy of Sciences, Beijing100049, China

11 ⁴Environmental Monitoring Center of Fujian, Fuzhou 350003, China

12 ⁵Fujian Key Laboratory of Severe Weather, Key Laboratory of Straits Severe Weather China
13 Meteorological Administration, Fuzhou 350007, China

14 ⁶Xiamen Institute of Environmental Science, Xiamen, China

15
16 *Corresponding authors. E-mail: Jinsheng Chen (jschen@iue.ac.cn); Youwei Hong
17 (ywhong@iue.ac.cn)

18
19 **Key Points:**

- 20 • A shift of distribution patterns of O₃ concentrations in coastal cities of China in the
21 unprecedented hot summer of 2022 were investigated.
- 22 • Meteorological changes caused 15.6% increase in O₃ concentrations in southern coastal
23 cities and 3.34% decrease in northern coastal cities.
- 24 • Extreme heat events increase the difficulty of O₃ pollution mitigation, especially in the
25 coastal areas with low O₃ precursor's emissions.
26

27 **Abstract**

28 Surface ozone pollution under climate warming has become a serious environmental issue. In the
29 summer of 2022, abnormal warming spread over most of the Northern Hemisphere and resulted
30 in the abnormal increase in O₃ concentration. In this study, we focused on the coastal cities in
31 China and investigated the O₃ trends in July during 2015 to 2022. Four regions with different
32 locations and emission levels were selected for comparison. A significant increase of O₃
33 concentration in July 2022 were observed in the southern coastal cities (16.7-22.8 μg m⁻³) while
34 the opposite characteristics were found in the northern coastal cities (decrease of 0.26-2.18 μg m⁻³).
35 The results indicated various distribution patterns of the O₃ concentrations responded to heat
36 wave across China. The weakening of East Asian summer monsoon, extension of the western
37 Pacific subtropical high, significant warming, stronger solar radiation, lower relative humidity,
38 less rainfall and sinking motion of atmosphere in 2022 were beneficial for O₃ generation and
39 accumulation in the southern coastal areas. Meteorological changes during July 2022 could lead
40 to an increase of 15.6% in O₃ concentrations in southern coastal cities compared to that in 2015-
41 2021, based on the analysis of machine learning. Air temperature was the main contributor to
42 high O₃ concentrations in the coast of Fujian province, while other coastal cities depended on
43 relative humidity. This study indicated the challenge of O₃ pollution control in coastal areas
44 under global warming, especially in extreme heat wave events.

45 **Plain Language Summary**

46 The variations of surface ozone are affected by emission levels and meteorological conditions.
47 China experienced a record-breaking hot summer in 2022 and abnormal increase in O₃
48 concentrations in the southern coastal cities. Compared with meteorological conditions from
49 2015 to 2021, the weakening of East Asian summer monsoon, extension of the western Pacific
50 subtropical high, significant warming, strong solar radiation, low relative humidity, less rainfall
51 and sinking motion of atmosphere in 2022 were beneficial for O₃ formation and accumulation in
52 the southern coastal cities. We furtherly applied a machine-learning based approach to evaluate
53 the meteorological impact on O₃ trends during 2015 to 2022, and found that the meteorological
54 changes in July 2022 resulted in an 15.6% increase of daytime O₃ concentrations in southern
55 coastal cities. O₃ variations in the coastal area of Fujian province are strongly dependent on air
56 temperature. This study implied the necessary for local governments to consider climate change
57 for mitigating O₃ pollution.

58 **1 Introduction**

59 Surface ozone (O₃), primarily generated through a series of complex photochemical
60 reaction involving carbon monoxide, volatile organic compounds (VOCs) and nitrogen oxides
61 (NO_x) in the troposphere, is an air pollutant that be harmful to both human health and ecosystems
62 (C. Li et al., 2022; Wang et al., 2022; Weng et al., 2022). Along with the global warming, heat
63 waves have occurred more frequently in most part of Europe, Asia and Australia along with the
64 ascendance of O₃ concentrations (Pu et al., 2017). Meteorological conditions accompanied with
65 heat waves, including sustained high temperature, strong solar radiation, weak wind speed and
66 little cloud coverage, could enhance O₃ production (Ma et al., 2019). Heat wave has gradually
67 become a common danger in the world (Zhang et al., 2023) and the risk of temperature-related
68 O₃ pollution may be greatly increased in the future. Although the important role of meteorology
69 in O₃ pollution under heat wave is widely acknowledged, its mechanisms and quantitative
70 contribution under extreme weather remains highly uncertain. Thus, it is vital to investigate the

71 meteorological impact and possible mechanisms leading to high O₃ levels in extreme weather
72 events.

73 The effectiveness of O₃ production is mainly controlled by not only the levels of
74 precursors emissions, but also meteorological conditions (Weng et al., 2022; Zhang et al., 2018).
75 Meteorological impacts on O₃ are attracting more attentions from researchers (Y. Dong et al.,
76 2020; Gao et al., 2021; Liu et al., 2019). It has been proved that meteorological factors could
77 have remarkable impact on O₃ concentrations, but temperature and solar radiation were indicated
78 to be the prevailing variables (Pu et al., 2017; Yin et al., 2019; Yu et al., 2019). Since O₃ levels
79 are significantly impacted by changes of precursor's emission and meteorological condition, it is
80 important to split the effect of meteorology and emissions while evaluating the O₃ trends.
81 Statistical analysis methods including Kolmogorov-Zurbenko (KZ) filter model (Ma et al., 2016;
82 Yin et al., 2019; Yu et al., 2019), multiple linear regression (MLR) (Han et al., 2020; Qian et al.,
83 2022) and machine learning (ML) (Vu et al., 2019; Wang et al., 2020; Weng et al., 2022) have
84 been widely used to study the meteorological impact on O₃ concentrations. It was suggested that
85 quantified meteorological contributions could vary regionally due to various climate conditions
86 along with the rapid but regionally imbalanced economic developments across China (C. Li et
87 al., 2022).

88 Over the last decade, the concentrations of ambient fine particulate matter (PM_{2.5}) in
89 China have been decreased since the successful implement of air pollution control policies (C. Li
90 et al., 2022; Yang et al., 2022b). However, O₃ concentrations increased, especially during
91 summer time when the local photochemical process is the strongest (Ma et al., 2019; Zhang et
92 al., 2018). This indicates the greater urgency for O₃ pollution control. In the summer of 2022,
93 abnormal warming spread over most of the Northern Hemisphere, with Europe and China
94 especially suffering from the record-breaking heat wave (Ma & Yuan, 2023; Zhang et al., 2023).
95 The lasting of high temperature has resulted in widespread O₃ pollution (Zheng et al., 2023).
96 This event provided an opportunity to study the response of O₃ concentrations to extremely high
97 temperatures and related circulations. The significant impact of meteorological conditions on O₃
98 variabilities in coastal areas has been confirmed in our previous studies, especially in the areas
99 with relatively low precursor's emissions (Ji et al., 2023), and this study aims to further explore
100 the impact mechanism of meteorological changes on O₃ pollution in different coastal cities.

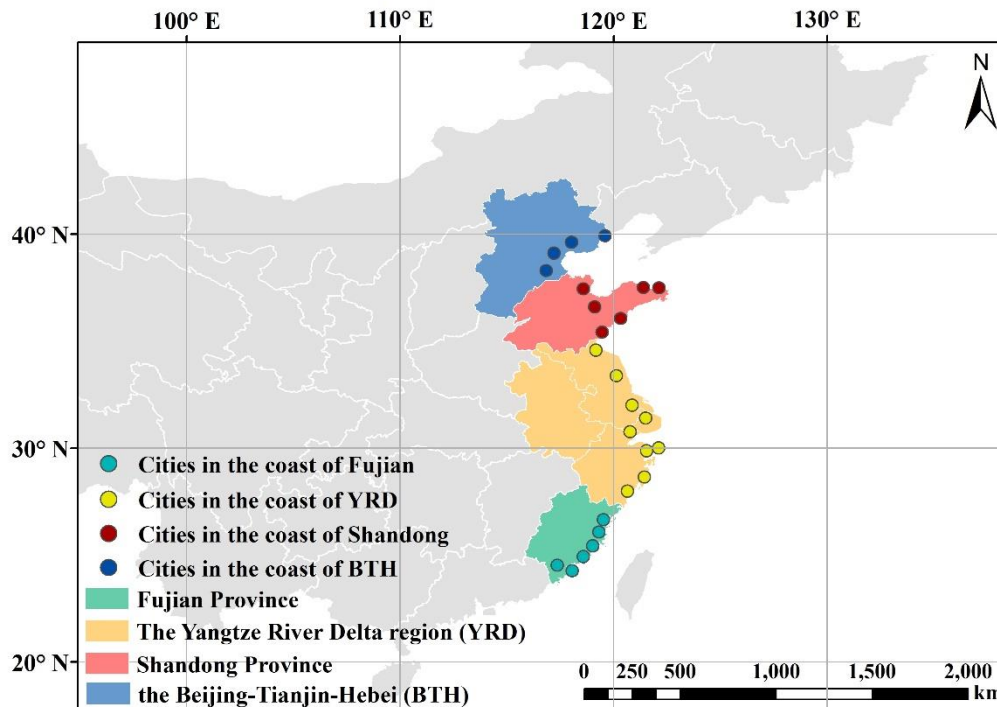
101 In this study, we characterized O₃ trends in July during 2015 to 2022 in four adjacent
102 coastal regions in Southern and Northern China. The exceptional O₃ variabilities and
103 meteorological conditions during the heat wave in 2022 were analyzed to study the
104 meteorological factors that possibly contributed to the high O₃ levels during the extremes. In
105 addition, a ML-based weather normalization was applied to assessing the meteorological
106 contribution on O₃ variabilities in coastal cities.

107 **2 Materials and Methods**

108 **2.1 Surface ozone and meteorological datasets**

109 In order to study the meteorological impact on O₃ pollution during heat waves in coastal
110 area, two southern coastal areas (the coast of Fujian Province (c-FJ) and the coast of Yangtze
111 River Delta region (c-YRD)) and two northern coastal areas (the coast of Shandong Peninsula (c-
112 SD) and Beijing-Tianjin-Hebei (c-BTH)) were selected for comparison. Totally 25 coastal cities
113 were picked as typical cities representative of the studied regions (Zhangzhou, Xiamen,

114 Quanzhou, Putian, Fuzhou and Ningde in c-FJ; Wenzhou, Taizhou, Ningbo, Zhoushan, Jiaxing,
 115 Shanghai, Nantong, Yancheng and Lianyungang in c-YRD; Rizhao, Qingdao, Weifang, Weihai,
 116 Yantai and Dongying in c-SD; Cangzhou, Tianjin, Tangshan and Qinhuangdao in c-BTH) and
 117 the data was averaged to obtain the O₃ concentrations and meteorological conditions regionally.
 118 The locations of the four regions are shown in Figure 1 and the precursor's emission levels are
 119 listed in Table S1. The BTH and the YRD are usually regarded as one of the most densely
 120 populated regions in China, and Fujian province is a southern coastal region with relatively low
 121 pollutants emission levels.



122

123 **Figure 1.** Geographic location of the studied area and cities.

124

125 Hourly ground-level O₃ concentrations used in this study were obtained from
 126 <https://quotsoft.net/air/> (last access: 24 March 2023) which is a mirror of the data from the
 127 Ministry of Ecology and Environment (MEE) of China. The meteorological factors including
 128 temperature at 2 m (T₂), relative humidity (RH), U and V wind components at 10 m (U₁₀ and
 129 V₁₀, respectively), surface solar radiation downward (SSRD), sea level pressure (SLP), low cloud
 130 cover (LCC), precipitation (P), boundary layer height (BLH), vertical velocity and wind
 131 divergence were obtained from the European Centre for Medium-Range Weather Forecasts
 132 (ECMWF) ERA5 hourly reanalysis dataset with a spatial resolution of 0.25°×0.25°.

133 2.2 Weather Normalization

134 A weather normalization approach based on random forest (RF) was applied to decouple the
 135 effect of meteorological condition from the observed O₃ series and investigate the meteorological
 136 impact on O₃ variabilities investigate the meteorological impact on O₃ variabilities in each study
 137 region. It was implemented using the “rmweather” R package developed by Grange et al. (2018),

138 aiming to develop a statistical model that predicts O₃ concentrations under constant
139 meteorological conditions. RF models which used O₃ concentrations as the dependent variable
140 for each of the 4 study regions were grown. All RF models used the same explanatory variables
141 to predict hourly O₃ concentrations. We used the hourly meteorological data including
142 temperature at 2 m (T₂), relative humidity (RH), U and V wind components at 10 m (U₁₀ and
143 V₁₀, respectively), surface solar radiation downward (SSRD), sea level pressure (SLP), low cloud
144 cover (LCC), precipitation (P) and boundary layer height (BLH) between 6:00 to 18:00 in July
145 during 2015 to 2022 as input data for the model. It has been proved that the data of these hours is
146 sufficient to cover the daytime hours when O₃ is produced by photochemical process (Weng et
147 al., 2022). In addition, time variables were added to the explanatory variables as proxies of time-
148 related variables such as emission intensity. We applied Unix time (number of seconds since 1
149 January 1970) as the linear trend component, Julian day (day of the year) as the seasonal
150 component, day of the week as the weekly component and hour of the day as the diel-cycle
151 component.

152 Training of the models was conducted on 80% of the input data and the remaining 20% was
153 used to test the model. The hyper-parameters for all the models were consistent with previous
154 studies: the number of variables used to grow a tree was set to three, the number of trees within a
155 forest was set to 300 and the minimum size of terminal nodes was five (Grange et al., 2018;
156 Wang et al., 2020). For O₃ series in each study region, the weather normalization was achieved
157 by repeatedly sampling and predicting using RF models. After weather normalization, the O₃
158 trends that are solely caused by the emission changes were singled out and identified as “de-
159 weathered O₃”, then the difference with the observed O₃ can represent the meteorological impact
160 (C. Li et al., 2022). The de-weathered concentrations at a particular hour were calculated by
161 averaging 1000 predictions from the meteorological factors (excluding all time variables)
162 randomly resampled from the whole period. Thus, this presented the O₃ trend disentangling the
163 meteorological impacts.

164 2.3 Definition of heat wave, O₃ standard-exceeding days and East Asian summer 165 monsoon index

166 Heat waves can be broadly defined as a period of consecutive days with higher air
167 temperature than normal. World Meteorological Organization (WMO) suggests that daily
168 maximum air temperature higher than 32 °C and last for more than three days can be regarded as
169 heat waves (Pu et al., 2017). The heat waves episodes in this study were defined according to this
170 standard.

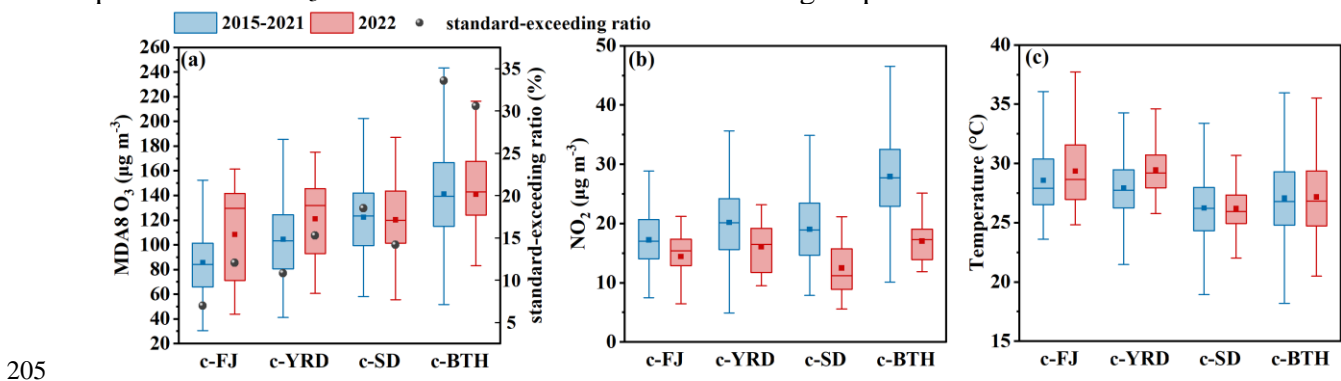
171 O₃ standard-exceeding days were defined as days when the maximum daily 8-h average
172 (MDA8) O₃ concentrations of a city were above 160 µg m⁻³, according to the Technical
173 Regulation on Ambient Air Quality Index of China publisher by the Ministry of Environmental
174 Protection of China in 2012 (GB 3095-2012) (Yueming Dong et al., 2020; Yan et al., 2023).

175 To achieve a comprehensive indication of the East Asian summer monsoon (EASM)
176 features, we calculated the EASM index based on the rules suggested by Wang et al. (2008). It is
177 defined by the U_{850} in (22.5° - 32.5° N, 110° E-140° E) minus U_{850} in (5° - 15° N, 90° E-130° E).
178 Here, U_{850} presents the zonal winds in 850 hPa.

179 **3 Results and discussion**

180 3.1 Overview of surface ozone and temperature

181 Fig. 2 shows the comparisons of MDA8 O₃, average O₃ standard-exceeding ratio, daily
 182 mean NO₂ and hourly air temperature in July from 2015 to 2021 and 2022 in the four coastal
 183 regions. The O₃ concentrations in c-BTH and c-YRD with high population density and economic
 184 development level were higher than those in c-FJ. A significant increase of both O₃
 185 concentrations and air temperature in July 2022 were observed in the southern coastal cities (c-FJ
 186 and c-YRD). The monthly average MDA8 O₃ during 2015-2021 are shown in Fig. S1 and it is
 187 found that the monthly variations of O₃ concentrations in the southern coastal cities tended to
 188 show a “double-peak pattern”, with peak values occurring in Spring and Autumn, while a
 189 “single-peak pattern” that peaked in Summer was found in the northern coastal cities (c-SD and
 190 c-BTH) (Fig. S1). The O₃ concentrations were relatively low in July in the southern coastal cities
 191 during the past few years. However, the average MDA8 O₃ in July 2022 ($108.42 \pm 38.79 \mu\text{g m}^{-3}$
 192 in c-FJ and $121.13 \pm 33.26 \mu\text{g m}^{-3}$ in c-YRD) increased significantly, compared to those during
 193 2015-2021 ($85.65 \pm 26.35 \mu\text{g m}^{-3}$ in c-FJ and $104.48 \pm 32.02 \mu\text{g m}^{-3}$ in c-YRD), even
 194 approaching the highest concentration in the Spring ($103.57 \pm 32.02 \mu\text{g m}^{-3}$ in April in c-FJ and
 195 $127.17 \pm 27.26 \mu\text{g m}^{-3}$ in May in c-YRD). The O₃ standard-exceeding ratios raised from 9.44%
 196 to 14.5% in c-FJ and 13.3% to 17.7% in c-YRD. In the northern coastal cities, the average
 197 MDA8 O₃ in July 2022 showed a slight decrease ($-2.18 \mu\text{g m}^{-3}$ in c-SD and $-0.26 \mu\text{g m}^{-3}$ in c-
 198 BTH), compared to those from 2015 to 2021. The O₃ standard-exceeding ratios decreased from
 199 21.0% to 16.7% in c-SD and 36.1% to 33.1% in c-BTH. A decrease of NO₂ (one of the important
 200 precursors of O₃) concentrations was observed in all the four regions (Fig. 2). Temperature in
 201 southern coastal cities showed a significant increase compared to that during 2015-2021, while
 202 the temperature changed slightly in the northern coastal cities. These may indicate the important
 203 role of meteorological conditions on O₃ variations in coastal areas and the various distribution
 204 patterns of the O₃ concentrations under different heating amplitudes.

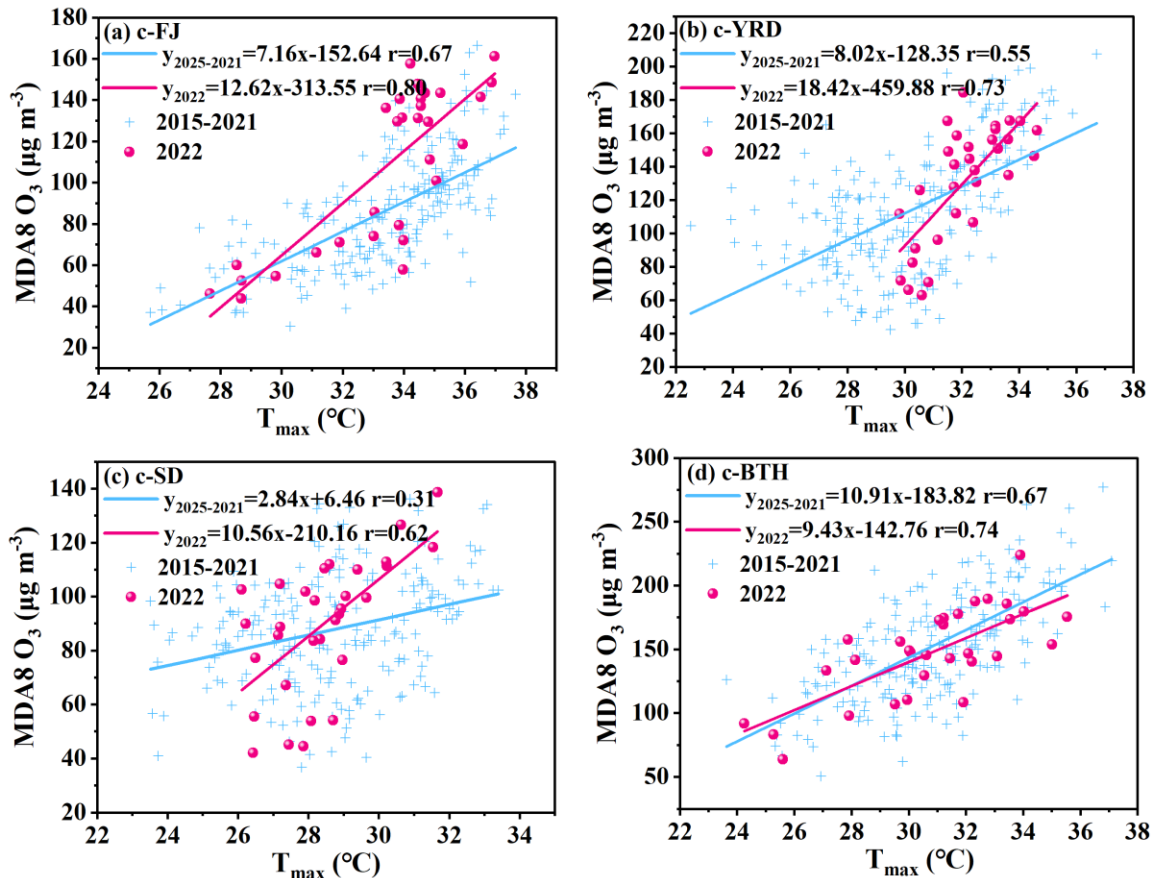


206 **Figure 2.** Comparisons of MDA8 O₃ and standard-exceeding ratio (a), daily mean NO₂ (b) and
 207 hourly air temperature (c) in July from 2015 to 2021 and 2022 in the coastal regions.

208
 209 We furtherly investigated the daily MDA8 O₃ concentrations, max temperature, average
 210 wind speed and total precipitation in July 2022 in the four regions are shown in Fig. S2. It was
 211 indicated that the temperature in c-FJ and c-YRD were much higher than that in c-SD and c-
 212 BTH. There were 24 and 20 days of heat wave in c-FJ and c-YRD, respectively, with daily
 213 maximum temperature higher than 32 °C. The O₃ concentrations in c-SD and c-BTH showed

214 more obvious fluctuations. High O₃ concentrations tended to occur during the periods of high
 215 temperature, weak wind speed and less precipitation. Precipitation could have a strong
 216 scavenging effect on O₃, thereby, the more precipitation in northern coastal cities responsible for
 217 the decrease of O₃ concentrations. Meanwhile, the extremely high temperature and stagnant
 218 conditions in southern coastal cities were beneficial for the generation and accumulation of O₃.

219 The correlation coefficients between MDA8 O₃ and daily maximum 2 m temperature in all
 220 the four regions show significant increase in 2022, compared to that from 2015 to 2021 (Fig. 3).
 221 The correlation coefficient in 2022 in c-FJ ($r=0.80$) was obviously higher than that from 2015 to
 222 2021 ($r=0.67$) and those in other regions ($r=0.73$ in c-YRD, $r=0.62$ in c-SD and $r=0.74$ in c-
 223 BTH), suggesting the significant influence of temperature on O₃ varieties. The regression slope
 224 in southern coastal cities in 2022 ($12.62 \mu\text{g m}^{-3} \text{ } ^\circ\text{C}^{-1}$ in c-FJ and $18.42 \mu\text{g m}^{-3} \text{ } ^\circ\text{C}^{-1}$ in c-YRD)
 225 were higher than that in 2015-2021 ($7.16 \mu\text{g m}^{-3} \text{ } ^\circ\text{C}^{-1}$ in c-FJ and $8.02 \mu\text{g m}^{-3} \text{ } ^\circ\text{C}^{-1}$ in c-YRD) and
 226 that in northern coastal cities. The results demonstrated the large impacts of temperature on O₃
 227 concentrations under the heat wave of 2022 in southern coastal cities. The observed abnormal O₃
 228 concentrations made the distribution patterns different, which might be associated with the
 229 intensified heat wave along with the related atmospheric circulations and meteorological
 230 anomalies.



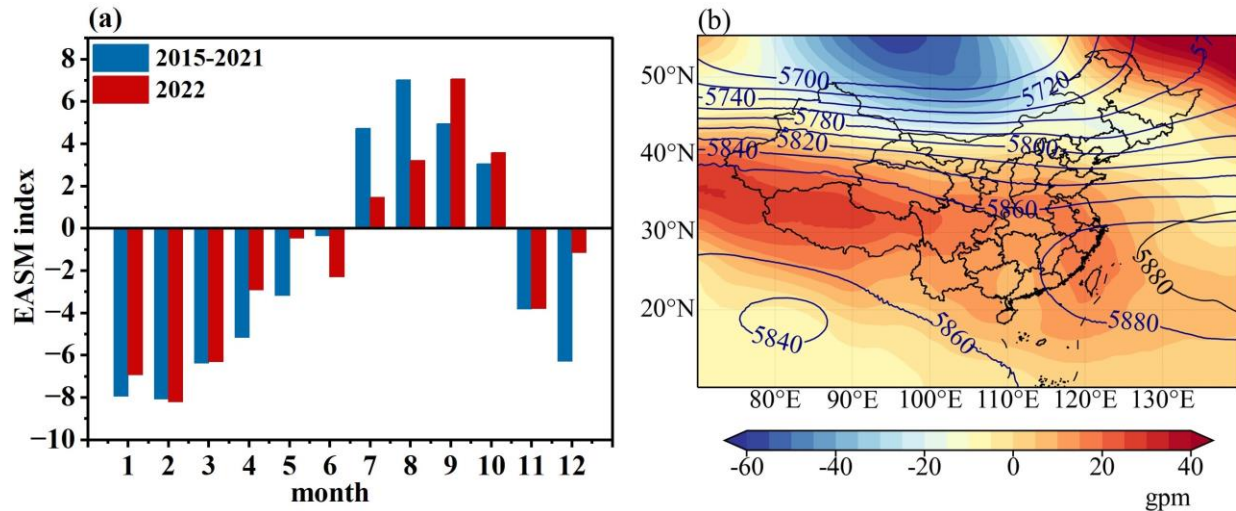
231
 232 **Figure 3.** The correlations between MDA8 O₃ and daily maximum temperature during 2015 to
 233 2021 and 2022 in the four regions.
 234

235 3.2 Meteorological contributions to O₃ variations

236 3.2.1 Climate and synoptic conditions

237 Climate in coastal area of China is significantly dominated by Asian monsoon system (He et
238 al., 2007). On seasonal to inter-annual scales, the East Asian summer monsoon (EASM) was
239 found to have a close link with O₃ concentrations over coastal regions of China (Zhou et al.,
240 2013). The EASM index was calculated and shown in Fig. 4(a). It is indicated that the EASM
241 index tended to be positive during summer and negative during other seasons, reaching the max
242 in August from 2015 to 2021. The EASM brings clean, warm and humid air from the ocean to
243 eastern (Zhou et al., 2022). A strong EASM year has been proved to be associated with the
244 abundant rainfall in southern China during June and July (Wu et al., 2008) and more northward
245 transport of pollutants induced by strong southerly winds (Xie et al., 2016). These may explain
246 the lower O₃ concentrations in summer in the past few years in the southern coastal cities.
247 However, a significantly weakening of EASM (Fig. 4(a)) and southwesterly winds (Fig. S3)
248 were observed in July 2022, which made the southern coastal areas experience hot, sunny and
249 stable weather at the time. The decrease of precipitation and weakening of southwesterly winds
250 over southern China could reduce the dilution of pollutants and lead to an anomalous O₃ flux
251 convergence in the southern areas (Xie et al., 2016; Yang et al., 2022a).

252 As one of the most important components of EASM, the western Pacific subtropical high
253 (WPSH) also plays a key role in meteorological conditions in Southern China during the
254 monsoon season (Zhao & Wang, 2017). The WPSH is the most direct circulation system that be
255 responsible for the heat wave. As shown in Fig. 4(b), the geopotential height at 500 hPa in 2022
256 was higher than those from 2015 to 2021 around the country. The WPSH ridge tended to be
257 defined as the line within the range of 5880 gpm and it was usually located over the ocean (Mao
258 et al., 2020). However, the abnormal extension was found in July of 2022, even adjoined
259 together with the Iran high (Lu et al., 2023). It was found that the WPSH covered the southern
260 coastal cities and contributed to heat wave via compression of sinking air, enhancement of solar
261 radiation and modulation of East Asian monsoon rain belt (Lu et al., 2023; Zhang et al., 2023).
262 These could promote the generation and accumulation of O₃ in the southern coastal cities, and
263 the details will be discussed in section 3.2.2. In addition, the movement of WPSH over the
264 southern coastal cities strengthened the westerly winds and a convergence of westerly and
265 southerly winds was found near the coastline (Fig. S3). This may also enhance the local
266 accumulation of O₃.



267

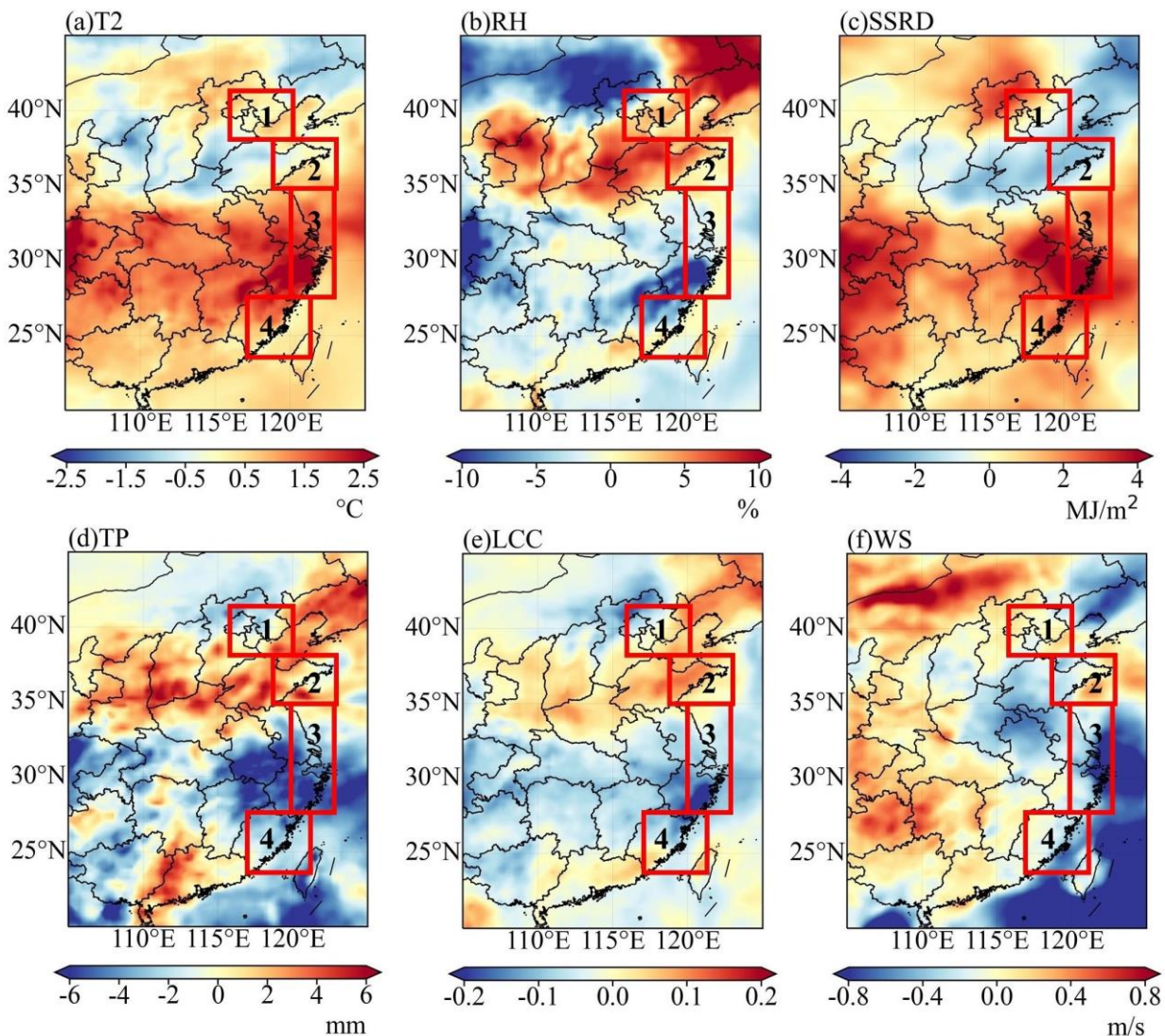
268 **Figure 4.** Comparison of EASM index between 2015-2021 and 2022 (a) and the changes of
 269 geopotential height at 500 hPa in 2022 compared with those from 2015 to 2021(b). The black
 270 lines represent the geopotential height in 2022 and the blue lines represent the average values of
 271 the geopotential height from 2015 to 2021.

272

273 3.2.2 Local meteorological conditions

274 To explore the changes on local meteorological condition and the underlying mechanisms
 275 that may be responsible for the high O_3 concentration in the southern coastal areas during the
 276 heat wave of 2022, we quantify the changes in various local meteorological factors in July
 277 between 2015-2021 and 2022 (Fig. 5). Most regions in China showed increase of air temperature
 278 at 2 m, and the highest anomalies occurred in YRD, which could be higher than 2.5 °C.
 279 However, the coastal areas of BTH and Shandong province showed slight increase of
 280 temperature, even negative anomalies. In addition, reduced relative humidity, strong solar
 281 radiation, less precipitation, less cloud cover and weak wind speed in southern coastal area were
 282 observed. Fig. S4 showed the difference of the average temperature, vertical velocity and wind
 283 divergence from 117°N to 122°N in July between 2022 and 2015-2021. Under the control of
 284 abnormally strong WPSH and record-breaking heat, the atmosphere in most of southern coastal
 285 cities were dominated by sinking motion. The vertical velocity was higher than that from 2015 to
 286 2021 under 500 hPa (Fig. S4(b)), indicating the stronger sinking motion under heat wave in
 287 southern coastal cities. Correspondingly, positive anomalies of divergence were observed in
 288 these areas and there existed two divergence centers at 1000-925 hPa between 20-28°N (Fig.
 289 S4(c)). The warming center between 850-700 hPa in c-FJ made the sinking airflow close to the
 290 surface. The vertical structure enhanced the stability of the atmosphere and favored the O_3 -
 291 benefiting sinking motion, usually leading to O_3 pollution episodes (Y. Li et al., 2022; Mao et al.,
 292 2020). These characteristics of meteorological conditions in southern coastal cities were
 293 favorable for the photochemical reaction but adverse to the removal and diffusion of O_3 , leading
 294 to the enhancement of O_3 pollution. The changes in meteorological factors in the northern coastal
 295 cities exhibited the opposite patterns, and this may explain the decrease in O_3 concentrations.

296



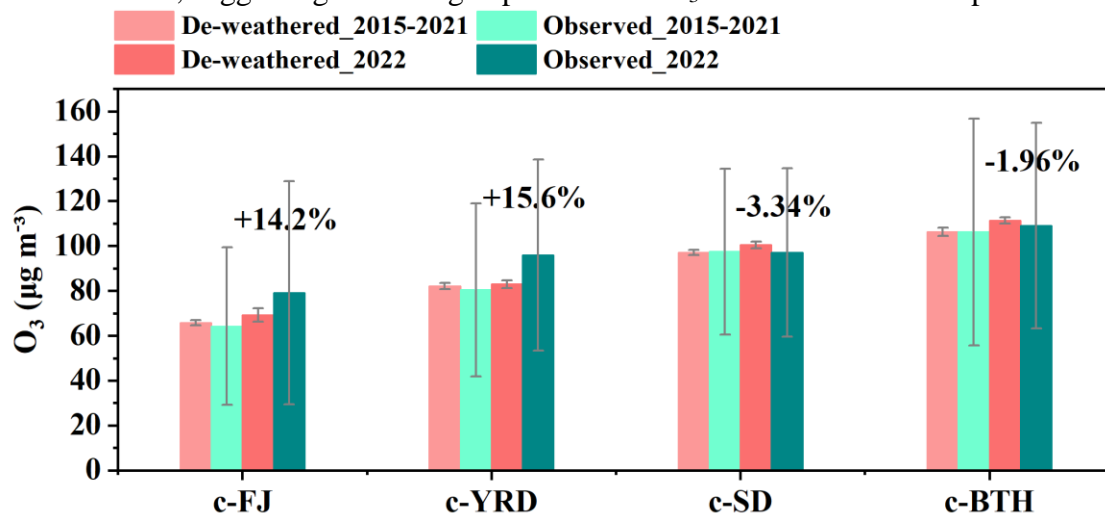
297

298 **Figure 5.** Spatial distribution in the difference between meteorological factors in July 2022 and
 299 the average value in July from 2015 to 2021. The meteorological factors included air temperature
 300 at 2 m (a), relative humidity at 1000 hPa (b), surface solar radiation downwards (c), total
 301 precipitation (d), low cloud cover (e) and wind speed (f). The red boxes represent the four
 302 regions: (1) c-BTH, (2) c-SD, (3) c-YRD and (4) c-FJ.

303 3.3 Evaluating the effectiveness of meteorological factors

304 The diurnal variations of O_3 concentrations during the daytime in July 2022 showed
 305 obvious increase in southern coastal cities, while a decrease could be found in the northern
 306 coastal cities (Fig. S5). These results indicated the differences in regional photochemical reaction
 307 processes, due to the changes of meteorological conditions. In order to quantify the impact of
 308 meteorological conditions to the O_3 variations during the daytime, the ML-based weather
 309 normalization was applied. Fig. 6 shows the observed and de-weathered O_3 concentrations in
 310 July in the four regions. It can be found that the de-weathered O_3 concentrations in July 2022

311 increased slightly in the four regions ($3.51 \mu\text{g m}^{-3}$ in c-FJ, $0.89 \mu\text{g m}^{-3}$ in c-YRD, $3.29 \mu\text{g m}^{-3}$ in
 312 c-SD and $4.98 \mu\text{g m}^{-3}$ in c-BTH), compared to the average values from 2015 to 2021. Compared to the
 313 de-weathered concentrations, the observed O_3 showed a significantly increase in the southern
 314 area ($9.85 \mu\text{g m}^{-3}$ in c-FJ and $12.98 \mu\text{g m}^{-3}$ in c-YRD). Thus, the unfavorable meteorological
 315 conditions during the heat wave led to 14.2% and 15.6% of O_3 increase in c-FJ and c-YRD,
 316 respectively. In the contrary, the O_3 concentrations in c-SD and c-BTH decreased $3.35 \mu\text{g m}^{-3}$
 317 (3.34%) and $2.18 \mu\text{g m}^{-3}$ (1.96%) due to the meteorological variabilities. The changes of
 318 meteorological conditions under heat wave in July 2022 made different impact on O_3 trends in
 319 the southern and northern coastal cities. These results indicated the possibility of distribution
 320 pattern changes under climate warming, which were consistent with the discussion of
 321 meteorological changes in section 3.2. In addition, although the enhancement of temperature in
 322 c-YRD was more significant, the meteorological contribution to the elevated O_3 was comparable
 323 to that in c-FJ, suggesting the strong dependence of O_3 variations on air temperature in c-FJ.



324

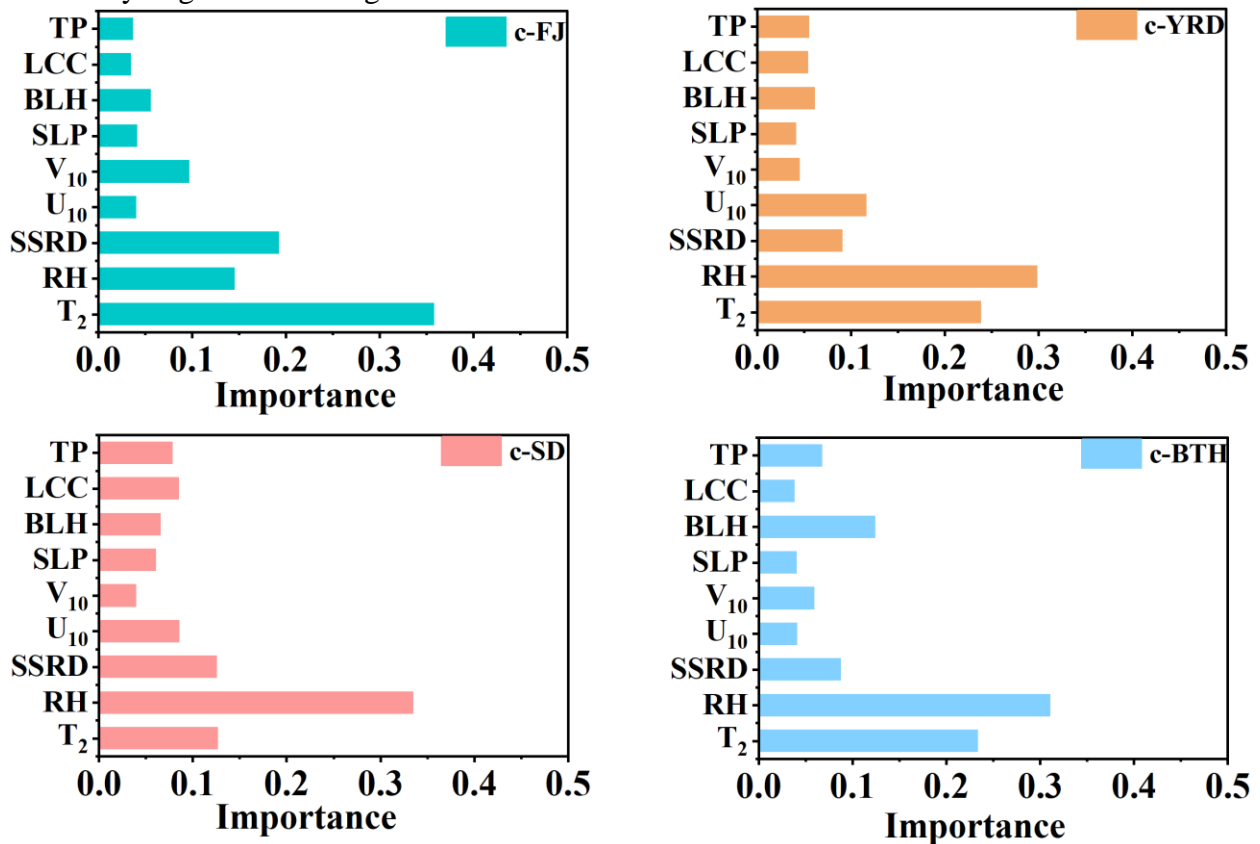
325 **Figure 6.** The observed O_3 concentrations and de-weathered O_3 concentrations in July from 2015
 326 to 2021 and in 2022.

327

328 We furtherly calculated the relative importance of each meteorological variables input into
 329 the models of weather normalization (Fig. 7). In c-FJ, air temperature is the most important
 330 variable (35.7%), followed by solar radiation (19.2%) and relative humidity (14.5%). The partial
 331 dependence plots of the most important variable in each region are shown in Fig. S8, which
 332 present the dependence of O_3 concentrations on one meteorological factor if all other factors are
 333 fixed at their average values. O_3 concentrations would increase with the range of temperature
 334 between $28^\circ\text{C} \sim 35^\circ\text{C}$ in c-FJ, due to the increased rates of photochemical reaction, biogenic and
 335 anthropogenic activities emissions (such as solvent evaporation) (Weng et al., 2022). As shown
 336 in Fig. S6, O_3 concentrations in c-FJ also could keep in high level under low RH, and high RH is
 337 beneficial for O_3 removal. In c-YRD, the O_3 trends were mainly affected by relative humidity
 338 (29.8%), air temperature (23.8%) and u-component of wind (11.6%), which implied the
 339 important roles of local photochemical reactions along with regional transport. The relationship
 340 between O_3 concentrations and RH in c-YRD was similar to that in c-FJ, but a decrease of O_3
 341 concentrations was found when air temperature increases from 24°C to 28°C . This indicated that
 342 the increase of O_3 concentrations in c-YRD not only depended on air temperature, but also
 343 affected by other factors. The O_3 concentrations tends to be high under low wind speed ($\sim 2\text{m/s}$)

344 which creates a more stagnant condition. West wind (positive values of U_{10}) could bring more air
 345 pollutants from inland areas and led to high O_3 concentrations, while east wind was favorable
 346 for the removal of O_3 due to the clean air masses from the sea (Weng et al., 2022). In c-SD,
 347 relative humidity showed the largest contribution to O_3 trends (33.5%), and O_3 concentrations in
 348 c-BTH mainly depended on relative humidity (31.1%), air temperature (23.4%) and boundary
 349 layer height (12.4%). The O_3 concentrations were enhanced with the increase of the boundary
 350 layer height, which associated with hot, sunny and deep convective boundary layer conditions in
 351 the daytime (Grange et al., 2018). Previous studies reported that O_3 variations in the relatively
 352 dry regions depended more on temperature and solar radiation instead of relative humidity
 353 (Weng et al., 2022). In this study, meteorological changes during the hot summer of 2022 led to
 354 high humidity and more precipitation in northern coastal areas (Fig. 5), which resulted in O_3
 355 variations in northern coastal areas were much different from southern coastal areas.

356 Therefore, the highest O_3 concentrations were observed when air temperature reached its
 357 maximum value in all the coastal cities, indicating the large possibility of O_3 pollution under heat
 358 waves. Under the heat wave conditions, the contribution of air temperature to high O_3
 359 concentrations in c-FJ was higher than those in other regions. This study implied that O_3
 360 concentrations in coastal areas with low O_3 precursors' emission levels could present strong
 361 sensitivity to global warming.



362

363 **Figure 7.** The relative importance of different meteorological factors in the four study areas in
 364 2022.

365

366 **4 Conclusions**

367 The impact of meteorological changes on O₃ concentrations in the coastal cities of China
368 under heat wave in summer of 2022 was evaluated. The O₃ trends in July during 2015 to 2022
369 were investigated in four coastal areas with different geolocations and emission magnitudes in
370 China. Compared to that during 2015-2021, a significant increase of O₃ concentrations
371 (16.7~22.8 μg m⁻³) in the southern coastal cities, while a slight decrease in the northern coastal
372 cities were observed. The results indicated a shift of distribution patterns of O₃ concentrations in
373 coastal cities of China in the unprecedented hot summer of 2022 and suggested the varied
374 mechanism O₃ concentrations responded to heat wave around the country. The enhancement of
375 O₃ concentration mainly occurred during the days with higher temperature, low wind speed and
376 less rainfall.

377 The year 2022 featured a weakened East Asian summer monsoon and abnormal extension
378 of the western Pacific subtropical high. Associated with the changes of climate and synoptic
379 conditions, the record-breaking warming, strong solar radiation, low relative humidity, less
380 rainfall and deep sinking motion of atmosphere in the southern coastal cities made a favorable
381 condition for the O₃ formations and accumulations.

382 According to the results of machine-learning based weather normalization, we found that
383 the unfavorable meteorological conditions in July 2022 could lead to a 15.6% increase in O₃
384 concentrations during the daytime in the southern coastal cities and a 3.34% decrease in the
385 northern coastal cities. Totally, air temperature, relative humidity, solar radiation, zonal wind and
386 boundary layer height could have overwhelming impact on the O₃ variations in coastal areas.
387 Heat wave made the meteorological condition and drivers of O₃ variations different across the
388 country. Air temperature was the main contributor in the coast of Fujian province (35.7%), while
389 the other areas depended on relative humidity (29.8%~33.5%). Although the enhancement of
390 temperature in c-YRD was more significant, c-FJ experienced the highest O₃ concentrations
391 ascend rate. This suggested large possibility of O₃ pollution under heat waves in the coastal areas
392 with lower precursor's emission. This study demonstrated the meteorological impact on O₃
393 concentrations enhancement during heat wave, and implied the challenge of mitigating O₃
394 pollution under global warming.

395 **Acknowledgments**

396 This work was funded by the National Natural Science Foundation of China (NO.
397 U22A20578 & 42277091), the Science and Technology Department of Fujian Province (NO.
398 2022L3025), the National Key Research and Development Program (NO. 2022YFC3700304),
399 and the Xiamen Atmospheric Environment Observation and Research Station of Fujian Province.
400

401 **Open Research**

402 A dataset for this paper can be accessed at (Ji et al., 2023).

403 **References**

- 404 Dong, Y., Li, J., Guo, J., Jiang, Z., Chu, Y., Chang, L., Yang, Y., & Liao, H. (2020). The impact
405 of synoptic patterns on summertime ozone pollution in the North China Plain. *Science of*
406 *The Total Environment*, 735. <https://doi.org/10.1016/j.scitotenv.2020.139559>
- 407 Dong, Y., Li, J., Guo, J., Jiang, Z., Chu, Y., Chang, L., Yang, Y., & Liao, H. (2020). The impact
408 of synoptic patterns on summertime ozone pollution in the North China Plain. *Sci Total*
409 *Environ*, 735, 139559. <https://doi.org/10.1016/j.scitotenv.2020.139559>
- 410 Gao, D., Xie, M., Liu, J., Wang, T., Ma, C., Bai, H., Chen, X., Li, M., Zhuang, B., & Li, S.
411 (2021). Ozone variability induced by synoptic weather patterns in warm seasons of 2014–
412 2018 over the Yangtze River Delta region, China. *Atmospheric Chemistry and Physics*,
413 21(8), 5847-5864. <https://doi.org/10.5194/acp-21-5847-2021>
- 414 Grange, S. K., Carslaw, D. C., Lewis, A. C., Boleti, E., & Hueglin, C. (2018). Random forest
415 meteorological normalisation models for Swiss PM₁₀; trend
416 analysis. *Atmospheric Chemistry and Physics*, 18(9), 6223-6239.
417 <https://doi.org/10.5194/acp-18-6223-2018>
- 418 Han, H., Liu, J., Shu, L., Wang, T., & Yuan, H. (2020). Local and synoptic meteorological
419 influences on daily variability in summertime surface ozone in eastern China.
420 *Atmospheric Chemistry and Physics*, 20(1), 203-222. [https://doi.org/10.5194/acp-20-203-](https://doi.org/10.5194/acp-20-203-2020)
421 [2020](https://doi.org/10.5194/acp-20-203-2020)
- 422 He, J., Ju, J., Wen, Z., Lü, J., & Jin, Q. (2007). A review of recent advances in research on Asian
423 monsoon in China. *Advances in Atmospheric Sciences*, 24(6), 972-992.
424 <https://doi.org/10.1007/s00376-007-0972-2>
- 425 Ji, X. (2023). Ozone concentrations and meteorological factors in coastal areas of China in July
426 of 2015-2022 [Data set]. Zenodo. <https://doi.org/10.5281/zenodo.8210811>
- 427 Ji, X., Hong, Y., Lin, Y., Xu, K., Chen, G., Liu, T., Xu, L., Li, M., Fan, X., Wang, H., Zhang, H.,
428 Chen, Y., Yang, C., Lin, Z., & Chen, J. (2023). Impacts of Synoptic Patterns and
429 Meteorological Factors on Distribution Trends of Ozone in Southeast China During
430 2015–2020. *Journal of Geophysical Research: Atmospheres*, 128(14), e2022JD037961.
431 <https://doi.org/https://doi.org/10.1029/2022JD037961>
- 432 Li, C., Zhu, Q., Jin, X., & Cohen, R. C. (2022). Elucidating Contributions of Anthropogenic
433 Volatile Organic Compounds and Particulate Matter to Ozone Trends over China.
434 *Environ Sci Technol*, 56(18), 12906-12916. <https://doi.org/10.1021/acs.est.2c03315>
- 435 Li, Y., Zhao, X., Deng, X., & Gao, J. (2022). The impact of peripheral circulation characteristics
436 of typhoon on sustained ozone episodes over the Pearl River Delta region, China.
437 *Atmospheric Chemistry and Physics*, 22(6), 3861-3873. [https://doi.org/10.5194/acp-22-](https://doi.org/10.5194/acp-22-3861-2022)
438 [3861-2022](https://doi.org/10.5194/acp-22-3861-2022)
- 439 Liu, J., Wang, L., Li, M., Liao, Z., Sun, Y., Song, T., Gao, W., Wang, Y., Li, Y., Ji, D., Hu, B.,
440 Kerminen, V.-M., Wang, Y., & Kulmala, M. (2019). Quantifying the impact of synoptic
441 circulation patterns on ozone variability in northern China from April to October 2013–
442 2017. *Atmospheric Chemistry and Physics*, 19(23), 14477-14492.
443 <https://doi.org/10.5194/acp-19-14477-2019>
- 444 Lu, R., Xu, K., Chen, R., Chen, W., Li, F., & Lv, C. (2023). Heat waves in summer 2022 and
445 increasing concern regarding heat waves in general. *Atmospheric and Oceanic Science*
446 *Letters*, 16(1). <https://doi.org/10.1016/j.aosl.2022.100290>
- 447 Ma, F., & Yuan, X. (2023). When Will the Unprecedented 2022 Summer Heat Waves in
448 Yangtze River Basin Become Normal in a Warming Climate? *Geophysical Research*
449 *Letters*, 50(4). <https://doi.org/10.1029/2022gl101946>

- 450 Ma, M., Gao, Y., Wang, Y., Zhang, S., Leung, L. R., Liu, C., Wang, S., Zhao, B., Chang, X., Su,
451 H., Zhang, T., Sheng, L., Yao, X., & Gao, H. (2019). Substantial ozone enhancement
452 over the North China Plain from increased biogenic emissions due to heat waves and land
453 cover in summer 2017. *Atmos. Chem. Phys.*, *19*(19), 12195-12207.
454 <https://doi.org/10.5194/acp-19-12195-2019>
- 455 Ma, Z., Xu, J., Quan, W., Zhang, Z., Lin, W., & Xu, X. (2016). Significant increase of surface
456 ozone at a rural site, north of eastern China. *Atmospheric Chemistry and Physics*, *16*(6),
457 3969-3977. <https://doi.org/10.5194/acp-16-3969-2016>
- 458 Mao, J., Wang, L., Lu, C., Liu, J., Li, M., Tang, G., Ji, D., Zhang, N., & Wang, Y. (2020).
459 Meteorological mechanism for a large-scale persistent severe ozone pollution event over
460 eastern China in 2017. *J Environ Sci (China)*, *92*, 187-199.
461 <https://doi.org/10.1016/j.jes.2020.02.019>
- 462 Pu, X., Wang, T. J., Huang, X., Melas, D., Zanis, P., Papanastasiou, D. K., & Poupkou, A.
463 (2017). Enhanced surface ozone during the heat wave of 2013 in Yangtze River Delta
464 region, China. *Sci Total Environ*, *603-604*, 807-816.
465 <https://doi.org/10.1016/j.scitotenv.2017.03.056>
- 466 Qian, J., Liao, H., Yang, Y., Li, K., Chen, L., & Zhu, J. (2022). Meteorological influences on
467 daily variation and trend of summertime surface ozone over years of 2015-2020:
468 Quantification for cities in the Yangtze River Delta. *Sci Total Environ*, *834*, 155107.
469 <https://doi.org/10.1016/j.scitotenv.2022.155107>
- 470 Vu, T. V., Shi, Z., Cheng, J., Zhang, Q., He, K., Wang, S., & Harrison, R. M. (2019). Assessing
471 the impact of clean air action on air quality trends in Beijing using a machine learning
472 technique. *Atmospheric Chemistry and Physics*, *19*(17), 11303-11314.
473 <https://doi.org/10.5194/acp-19-11303-2019>
- 474 Wang, B., Wu, Z., Li, J., Liu, J., Chang, C.-P., Ding, Y., & Wu, G. (2008). How to Measure the
475 Strength of the East Asian Summer Monsoon. *Journal of Climate*, *21*(17), 4449-4463.
476 <https://doi.org/https://doi.org/10.1175/2008JCLI2183.1>
- 477 Wang, T., Xue, L., Feng, Z., Dai, J., Zhang, Y., & Tan, Y. (2022). Ground-level ozone pollution
478 in China: a synthesis of recent findings on influencing factors and impacts.
479 *Environmental Research Letters*, *17*(6), 063003. [https://doi.org/10.1088/1748-](https://doi.org/10.1088/1748-9326/ac69fe)
480 [9326/ac69fe](https://doi.org/10.1088/1748-9326/ac69fe)
- 481 Wang, Y., Wen, Y., Wang, Y., Zhang, S., Zhang, K. M., Zheng, H., Xing, J., Wu, Y., & Hao, J.
482 (2020). Four-Month Changes in Air Quality during and after the COVID-19 Lockdown
483 in Six Megacities in China. *Environmental Science & Technology Letters*, *7*(11), 802-
484 808. <https://doi.org/10.1021/acs.estlett.0c00605>
- 485 Weng, X., Forster, G. L., & Nowack, P. (2022). A machine learning approach to quantify
486 meteorological drivers of ozone pollution in China from 2015 to 2019. *Atmospheric*
487 *Chemistry and Physics*, *22*(12), 8385-8402. <https://doi.org/10.5194/acp-22-8385-2022>
- 488 Wu, G., Ding, Y., Chang, C.-P., Liu, J., Li, J., Wu, Z., & Wang, B. (2008). How to Measure the
489 Strength of the East Asian Summer Monsoon. *Journal of Climate*, *21*(17), 4449-4463.
490 <https://doi.org/10.1175/2008jcli2183.1>
- 491 Xie, X., Wang, H., Liu, X., Li, J., Wang, Z., & Liu, Y. (2016). Distinct effects of anthropogenic
492 aerosols on the East Asian summer monsoon between multidecadal strong and weak
493 monsoon stages. *Journal of Geophysical Research: Atmospheres*, *121*(12), 7026-7040.
494 <https://doi.org/10.1002/2015jd024228>

- 495 Yan, Y., Wang, X., Huang, Z., Qu, K., Shi, W., Peng, Z., Zeng, L., Xie, S., & Zhang, Y. (2023).
496 Impacts of synoptic circulation on surface ozone pollution in a coastal eco-city in
497 Southeastern China during 2014-2019. *J Environ Sci (China)*, 127, 143-157.
498 <https://doi.org/10.1016/j.jes.2022.01.026>
- 499 Yang, Y., Li, M., Wang, H., Li, H., Wang, P., Li, K., Gao, M., & Liao, H. (2022a). ENSO
500 modulation of summertime tropospheric ozone over China. *Environmental Research*
501 *Letters*, 17(3). <https://doi.org/10.1088/1748-9326/ac54cd>
- 502 Yang, Y., Li, M., Wang, H., Li, H., Wang, P., Li, K., Gao, M., & Liao, H. (2022b). ENSO
503 modulation of summertime tropospheric ozone over China. *Environmental Research*
504 *Letters*, 17(3), 034020. <https://doi.org/10.1088/1748-9326/ac54cd>
- 505 Yin, C., Deng, X., Zou, Y., Solmon, F., Li, F., & Deng, T. (2019). Trend analysis of surface
506 ozone at suburban Guangzhou, China. *Sci Total Environ*, 695, 133880.
507 <https://doi.org/10.1016/j.scitotenv.2019.133880>
- 508 Yu, Y., Wang, Z., He, T., Meng, X., Xie, S., & Yu, H. (2019). Driving factors of the significant
509 increase in surface ozone in the Yangtze River Delta, China, during 2013–2017.
510 *Atmospheric Pollution Research*, 10(4), 1357-1364.
511 <https://doi.org/10.1016/j.apr.2019.03.010>
- 512 Zhang, D., Chen, L., Yuan, Y., Zuo, J., & Ke, Z. (2023). Why was the heat wave in the Yangtze
513 River valley abnormally intensified in late summer 2022? *Environmental Research*
514 *Letters*, 18(3). <https://doi.org/10.1088/1748-9326/acba30>
- 515 Zhang, J., Gao, Y., Luo, K., Leung, L. R., Zhang, Y., Wang, K., & Fan, J. (2018). Impacts of
516 compound extreme weather events on ozone in the present and future. *Atmos. Chem.*
517 *Phys.*, 18(13), 9861-9877. <https://doi.org/10.5194/acp-18-9861-2018>
- 518 Zhao, Z., & Wang, Y. (2017). Influence of the West Pacific subtropical high on surface ozone
519 daily variability in summertime over eastern China. *Atmospheric Environment*, 170, 197-
520 204. <https://doi.org/10.1016/j.atmosenv.2017.09.024>
- 521 Zheng, H., Kong, S., He, Y., Song, C., Cheng, Y., Yao, L., Chen, N., & Zhu, B. (2023).
522 Enhanced ozone pollution in the summer of 2022 in China: The roles of meteorology and
523 emission variations. *Atmospheric Environment*, 301.
524 <https://doi.org/10.1016/j.atmosenv.2023.119701>
- 525 Zhou, D., Ding, A., Mao, H., Fu, C., Wang, T., Chan, L. Y., Ding, K., Zhang, Y., Liu, J., Lu, A.,
526 & Hao, N. (2013). Impacts of the East Asian monsoon on lower tropospheric ozone over
527 coastal South China. *Environmental Research Letters*, 8(4), 044011.
528 <https://doi.org/10.1088/1748-9326/8/4/044011>
- 529 Zhou, Y., Yang, Y., Wang, H., Wang, J., Li, M., Li, H., Wang, P., Zhu, J., Li, K., & Liao, H.
530 (2022). Summer ozone pollution in China affected by the intensity of Asian monsoon
531 systems. *Science of The Total Environment*, 849, 157785.
532 <https://doi.org/https://doi.org/10.1016/j.scitotenv.2022.157785>
533